The EMBO Journal (2010) 29, 3470–3483 | © 2010 European Molecular Biology Organization | All Rights Reserved 0261-4189/10
www.embojournal.org

THE EMBO JOURNAL

Dishevelled, a Wnt signalling component, is involved in mitotic progression in cooperation with Plk1

Koji Kikuchi[1], Yohei Niikura[2], Katsumi Kitagawa[2] and Akira Kikuchi[1,*]

[1]Department of Molecular Biology and Biochemistry, Graduate School of Medicine, Osaka University, Suita, Japan and [2]Center for Childhood Cancer, The Research Institute, Nationwide Children's Hospital, Columbus, OH, USA

Wnt signalling is known to promote G1/S progression through the stimulation of gene expression, but whether this signalling regulates mitotic progression is not clear. Here, the function of dishevelled 2 (Dvl2), which transmits the Wnt signal, in mitosis was examined. Dvl2 localized to the spindles and spindle poles during mitosis. When cells were treated with nocodazole, Dvl2 was observed at the kinetochores (KTs). Dvl2 bound to and was phosphorylated at Thr206 by a mitotic kinase, Polo-like kinase 1 (Plk1), and this phosphorylation was required for spindle orientation and stable microtubule (MT)-KT attachment. Dvl2 was also found to be involved in the activation of a spindle assembly checkpoint (SAC) kinase, Mps1, and the recruitment of other SAC components, Bub1 and BubR1, to the KTs. However, the phosphorylation of Dvl2 by Plk1 was dispensable for SAC. Furthermore, Wnt receptors were involved in spindle orientation, but not in MT-KT attachment or SAC. These results suggested that Dvl2 is involved in mitotic progression by regulating the dynamics of MT plus-ends and the SAC in Plk1-dependent and -independent manners.

The EMBO Journal (2010) **29,** 3470–3483. doi:10.1038/emboj.2010.221; Published online 7 September 2010
Subject Categories: signal transduction; cell cycle
Keywords: dishevelled; microtubule plus end; mitosis; Plk1; Wnt signalling

Introduction

Wnt is a secreted ligand that is essential for animal development (Logan and Nusse, 2004). When Wnt acts on its cell-surface receptor, which consists of Frizzled (Fz) and low density lipoprotein receptor-related protein 5/6 (LRP5/6), cytoplasmic β-catenin is stabilized by release from the Axin complex, including glycogen synthase kinase 3 (GSK3) and adenomatous polyposis coli (APC) protein (Kikuchi *et al*, 2009; MacDonald *et al*, 2009). The accumulated β-catenin is translocated to the nucleus, in which it binds to transcription factor T-cell factor (Tcf)/lymphoid enhancer factor (Lef) and thereby stimulates the expression of various genes, such as c-Myc and cyclin D1. Therefore, Wnt/β-catenin signalling is known to promote G1/S progression. Interestingly, evidence has been accumulated that components of the Wnt/β-catenin pathway, such as β-catenin, APC, GSK3β, and Axin2, localize to the mitotic spindle or centrosomes and are involved in the regulation of mitotic progression (Kaplan *et al*, 2001; Hadjihannas *et al*, 2006; Bahmanyar *et al*, 2008; Fumoto *et al*, 2008; Izumi *et al*, 2008; McCartney and Näthke, 2008). Furthermore, it has been reported that LRP6 is efficiently phosphorylated by a mitotic cyclin Y-dependent protein kinase, Pftk, and that β-catenin-dependent transcription is enhanced in mitosis (Davidson *et al*, 2009). However, it is necessary to show that Wnts, their receptors, and dishevelled (Dvl), which binds directly to Fz, are involved in mitotic progression in order to confirm that Wnt signalling regulates mitosis.

Dvl mediates Wnt signalling to both the β-catenin-dependent and β-catenin-independent pathways (Wharton, 2003). It has been reported that Dvl is involved in asymmetric cell division in the early embryo of *Caenorhabditis elegans* (Walston *et al*, 2004). Cortical localization of Dvl at the posterior stimulates the disassembly of the complex containing Axin, APC, mitogen-activated protein kinase, and β-catenin and regulates the alignment and orientation of spindles in a Wnt-dependent manner. In mammals, Dvl has been shown to inhibit GSK3β locally, resulting in changes in the phosphorylation levels of GSK3β targets, such as the microtubule (MT)-associated protein 1B, thereby regulating the stabilization of MTs (Ciani *et al*, 2004). Furthermore, Dvl is required for Wnt-mediated MT reorganization and axon remodelling in growth cones (Purro *et al*, 2008). Thus, it is clear that Dvl is involved in cell division and MT stability. However, the mitotic functions of Dvl in mammals remain unclear.

Faithful segregation of chromosomes in mitosis is ensured by a fail-safe mechanism called by the spindle assembly checkpoint (SAC) (Cleveland *et al*, 2003; Musacchio and Salmon, 2007). When activated, the SAC inhibits the anaphase-promoting complex/cyclosome (APC/C) through interference with Cdc20, which blocks sister chromatid separation and mitotic exit until all pairs of opposing sister kinetochores (KTs) attach to MTs emanating from the two spindle poles (Musacchio and Salmon, 2007; Yu, 2007). The chromosomal domain responsible for mitotic inhibition through the SAC is the KT, and the KT localization of SAC components contributes to generate the SAC signal. A mitotic checkpoint complex (MCC) that contains three SAC proteins, Mad2, BubR1, and Bub3, as well as Cdc20, binds to the APC/C and inhibits its ubiquitin-ligase activity on securin and cyclin B1. Besides MCC, other SAC components, serine/threonine kinases, including Mps1, Mad1, Bub1, and Aurora B, are likely to be required for the amplification of the SAC signal. Mps1 is an

*Corresponding author. Department of Molecular Biology and Biochemistry, Graduate School of Medicine, Osaka University, 2-2 Yamadaoka, Suita, Osaka 565-0871, Japan. Tel.: +81 6 6879 3411; Fax: +81 6 6879 3419; E-mail: akikuchi@molbiobc.med.osaka-u.ac.jp

Received: 2 March 2010; accepted: 6 August 2010; published online: 7 September 2010

important kinase that is autophosphorylated and activated during mitosis (Abrieu *et al*, 2001; Stucke *et al*, 2002; Liu *et al*, 2003; Vigneron *et al*, 2004; Kang *et al*, 2007; Jelluma *et al*, 2008a). The recruitment of SAC proteins to KTs is hierarchical, and Mps1 lies upstream. However, how Mps1 is activated is not known.

In addition to these SAC kinases, Polo-like kinase 1 (Plk1), which is a mitotic kinase and governs multiple events in mitosis, is also localized to the KTs as well as the centrosome (Arnaud *et al*, 1998; Petronczki *et al*, 2008). Plk1 is required for not only the establishment of a bipolar spindle and functional centrosomes, but also for their maintenance (Lane and Nigg, 1996; Casenghi *et al*, 2003; Oshimori *et al*, 2006). Therefore, depletion of Plk1 in human cells disrupts the formation of a proper bipolar spindle, and increases monopolar spindle (Sumara *et al*, 2004). In addition, Plk1 is also required for the formation of MT-KT attachment by its function on KT (Sumara *et al*, 2004; Lénárt *et al*, 2007).

To clarify the regulation of mitosis by Wnt signalling, we first studied the functions of Dvl in mitosis. It was found that Dvl2, one of the Dvl family members in mammals, bound to and was phosphorylated by Plk1. Plk1-dependent phosphorylation of Dvl2 was required for the appropriate spindle rotation and MT-KT attachment. It was further shown that Dvl2 is required for SAC activation. However, the phosphorylation of Dvl2 by Plk1 is dispensable for SAC activation. These results suggest that Dvl2 is involved in mitotic progression by regulating the dynamics of MT plus-ends and the SAC in mitosis in Plk1-dependent and -independent manners, respectively. Finally, the possibility that Wnts and their receptors, LRP6 and Fz2, are involved in mitotic progression is discussed.

Results

Dynamic localization of Dvl2 in mitosis

To examine the subcellular localization of Dvl2 in mitosis, green fluorescence protein (GFP)-Dvl2 was transiently expressed in HeLaS3 cells because it was difficult to detect endogenous Dvl2 using several kinds of anti-Dvl2 antibody immunocytochemically. Exogenous GFP-Dvl2 was expressed at levels similar to endogenous Dvl2 (Supplementary Figure S1A). When cells entered into mitosis, GFP-Dvl2 localized to the spindle poles and was highly concentrated there at metaphase, but the signal intensity of GFP-Dvl2 decreased in anaphase (Figure 1A). GFP-Dvl2 also localized to the spindles from prometaphase to anaphase (Figure 1A and B). In telophase, GFP-Dvl2 was concentrated at the cleavage furrow (Figure 1A). In an enlarged image, GFP-Dvl2 was observed to be associated with some of the KTs, which were recognized by anti-centromere antibody (ACA) (Figure 1B). When cells were treated with nocodazole to disrupt MTs, GFP-Dvl2 was detected on most of the KTs (Figure 1C), suggesting that Dvl2 localizes to the KTs when SAC is active.

Live-image analysis using U2OS cells stably expressing GFP-Dvl2 revealed that GFP-Dvl2 localizes to the spindle poles mainly, but it was difficult to detect the localization of GFP-Dvl2 to the KTs (Supplementary Figure S1B). Exogenous GFP-Dvl2 was expressed at two- to three-fold higher levels than endogenous Dvl2 level (Supplementary Figure S1A). The subcellular localization of Dvl2 in mitosis suggested that Dvl2 is involved in the regulation of the mitotic spindle.

Dvl2 forms a complex with and is phosporylated by Plk1

A slowly migrating band of Dvl2 on SDS–polyacrylamide gel electrophoresis (PAGE) was observed in mitotic HeLaS3 and U2OS cells, as compared with asynchronous, interphase, or G1/S phase cells (Figure 2A; Supplementary Figure S2A and C). This slowly migrating band disappeared after treatment with alkaline phosphatase (AP) (Figure 2B), suggesting that Dvl2 is phosphorylated in mitosis. To examine whether the phosphorylation of Dvl2 depends on a Wnt ligand, Dickkopf1 (Dkk1), which suppresses Wnt signalling by downregulating Wnt receptor LRP6 (Niehrs, 2006; Yamamoto *et al*, 2008), was added to mitotic HeLaS3 cells. Dkk1 did not affect the mobility shift of Dvl2, suggesting that mitotic phosphorylation of Dvl2 is independent of Wnt and LRP6 (Supplementary Figure S2C).

Mitotic phosphorylation is often regulated by mitotic kinases such as cyclin-dependent protein kinase 1 (Cdk1), Plk1, and Aurora kinase. Dvl2 was immunoprecipitated with Plk1 at endogenous levels in mitosis (Figure 2C). However, Dvl2 did not form a complex with Cdk1 or Aurora A when they were overexpressed (Supplementary Figure S2D). In addition, the C-terminal region, including the Polo-box, of Plk1 interacted with Dvl2 (Supplementary Figure 3A), and the region (aa 354–423) between the PDZ and DEP domains of Dvl2 was required for binding to Plk1 (Supplementary Figure 3B). The DIX and PDZ domains are necessary for the Wnt/β-catenin-dependent pathway, and the DEP domain mediates Wnt/β-catenin-independent pathway (Wharton, 2003). The aa 354–423 region of Dvl2 has a core consensus motif for Polo-box binding, Ser-pSer/pThr-Pro/X, such as Ser-Ser-Ser, Ser-Ser-Met, and Ser-Ser-Leu. It has been reported that Plk1 interacts with its substrates through the C-terminal Polo-box domain (Elia *et al*, 2003), and depletion of Plk1 using small-interfering RNA (siRNA) abolished mitotic phosphorylation of Dvl2 (Figure 2D), suggesting that Plk1 is involved in the mitotic phosphorylation of Dvl2.

Putative Plk1-phosphorylation sites, which were searched for using a group-based phosphorylation-scoring method (Xue *et al*, 2005), were conserved in Dvl2 from zebrafish to human (Supplementary Figure S4A). Dvl2 fused to maltose-binding protein (MBP-Dvl2) was phosphorylated by GST-Plk1, but not by an inactive kinase form (K82R) of Plk1 (Figure 2E). Notably, degradation forms of Dvl2, which might lack the C-terminal region of Dvl2, were phosphorylated by Plk1 (Figure 2E). Consistently, a deletion mutant lacking the C-terminal region, MBP-Dvl2(1–433), was also phosphorylated by GST-Plk1, but not by GST-Plk1^{K82R} (Supplementary Figure S4B).

To define the phosphorylation site(s) of Dvl2, a deletion mutant lacking the region containing residues 140–263, which includes several putative Plk1-phosphorylation sites, was generated from MBP-Dvl2(1–433) (MBP-Dvl2(1–433)$^{\Delta 140-263}$). MBP-Dvl2(1–433)$^{\Delta 140-263}$ was not phosphorylated by GST-Plk1 (Figure 2F). Putative-phosphorylation sites for Plk1, T206, T216, and T260 were replaced with alanine in the construct MBP-Dvl2(140–358) (Supplementary Figure S4A). S227 and S228, which are mitotic-phosphorylation sites reported previously (Dephoure *et al*, 2008), were also replaced with alanine in the construct (Supplementary Figure S4A). Among

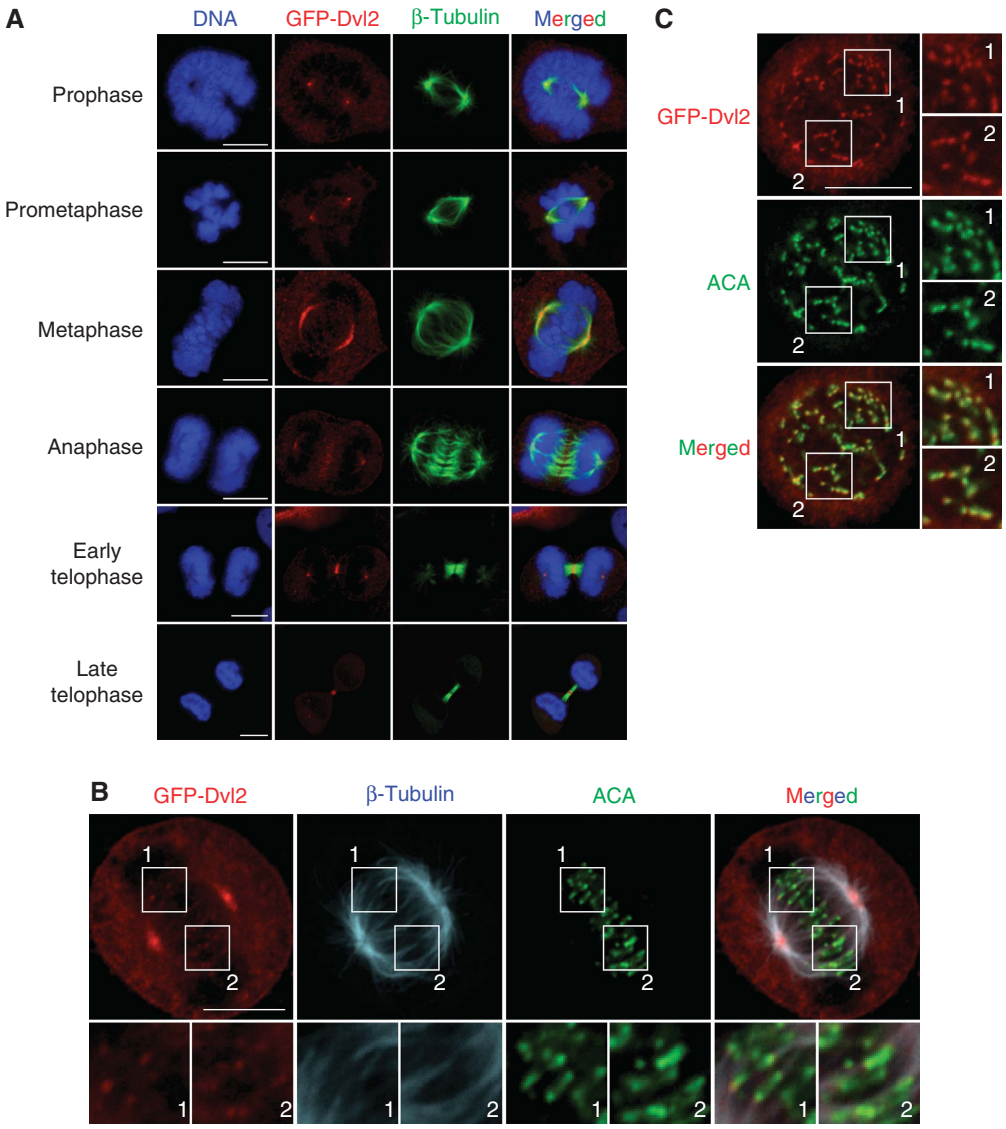

Figure 1 Subcellular localization of Dvl2 in mitosis. (**A**) HeLaS3 cells transiently expressing GFP-Dvl2 were stained for GFP-Dvl2 (red) or β-tubulin (green). DNA (blue) was stained with PI. (**B**) HeLaS3 cells expressing GFP-Dvl2 at metaphase were stained for β-tubulin (blue), ACA (a KT maker, green), or GFP-Dvl2 (red). (**C**) HeLaS3 cells expressing GFP-Dvl2 were treated with 200 ng/ml nocodazole for 1 h to disrupt MTs. Cells were stained for GFP-Dvl2 (red) or ACA (green). The region in the white box is shown enlarged. Scale bars in (**A**), (**B**), and (**C**), 10 μm.

these Dvl2 mutants, only MBP-Dvl2(140–358)^{T206A} was not phosphorylated (Figure 2G; Supplementary Figure S4C), suggesting that Dvl2 is specifically phosphorylated at T206 by Plk1.

Dvl2 regulates spindle orientation

Depletion of Dvl2 in HeLaS3 cells affected neither bipolar formation nor the localization of Plk1 to the spindle poles in mitosis (Figure 3A; Supplementary Figure S5A), whereas depletion of other mitotic MAPs, such as Tpx2 and NuMA, disrupted bipolar formation (Andersen, 2000; Kline-Smith and Walczak, 2004). However, fibres of astral MTs, which are essential for spindle orientation, were reduced in Dvl2-depleted HeLaS3 cells (Figure 3A). Furthermore, time-lapse images of Dvl2-depleted cells showed that the cells fail to immediately gain adhesion to the substratum after cell division (Figure 3B; Supplementary Movies 1 and 2). Approximately 37% of Dvl2-depleted dividing cells (10/27) failed to gain adhesion and were overlapping with another adhered cell, whereas only 10% of control cells showed a similar phenotype (Figure 3B). When no other cell is adjacent to the dividing cell, Dvl2-depeleted cells still failed to gain adhesion (Supplementary Figure 5B).

This phenotype often comes from the abnormality of the attachment of astral MTs to the cell cortex, which induces spindle misorientation (Toyoshima and Nishida, 2007). Spindle misorientation includes rotation of the spindle axis within the cells and displacement of the spindles from the centre of the cells (Draviam *et al*, 2006). To examine the effects of Dvl2 on the spindle axis, Z-stack images were taken from 0.2 μm-thick sections of metaphase cells and the angle between the axis of a metaphase spindle and that of the substrate surface, which is termed the spindle angle (θ), was calculated (Figure 3C). The spindle angle was angled (median: 11.3°) in Dvl2-depleted HeLaS3 cells as compared with that in control cells (median: 5.52°)

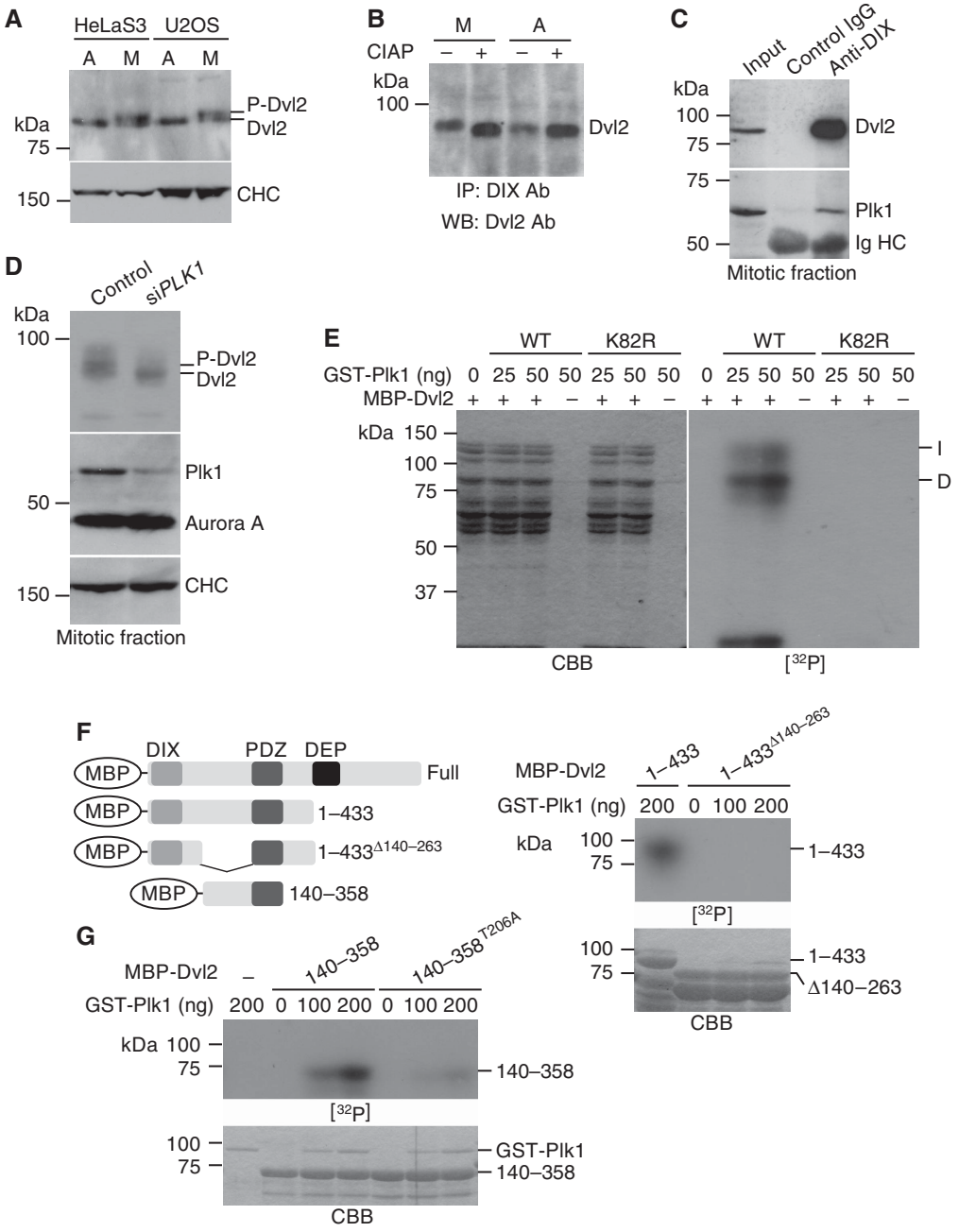

Figure 2 Dvl2 is phosphorylated by Plk1. (**A**) HeLaS3 or U2OS cells were arrested at prometaphase by treatment with 100 and 500 ng/ml nocodazole for 16 h, respectively. Cell lysates from asynchronous (A) or mitotic (M) cells were probed with anti-Dvl2 (Santa Cruz) or anti-clathrin heavy chain (CHC) antibody. (**B**) Lysates from asynchronous (A) or mitotic (M) HeLaS3 cells were immunoprecipitated using anti-DIX (Dvl) antibody, and the immunoprecipitates were treated with or without alkaline phosphatase (CIAP; TaKaRa) at 30°C for 15 min, followed by probing with anti-Dvl2 antibody. (**C**) Lysates from mitotic HeLaS3 cells were immunoprecipitated with control IgG or anti-DIX antibody. The immunoprecipitates were probed with anti-Dvl2 and anti-Plk1 antibodies. (**D**) Control or Plk1-depleted HeLaS3 cells were arrested at prometaphase by treating with nocodazole, and then the lysates were probed with the indicated antibodies. CHC and Aurora A were used as loading controls. (**E**) MBP-Dvl2 (250 ng of protein) was incubated with the indicated amounts of GST-Plk1 or GST-Plk1^{K82R} (K82R; a kinase inactive form) in kinase reaction buffer. 'I' and 'D' indicate intact MBP-Dvl2 and degraded MBP-Dvl2 protein, respectively. The samples were subjected to SDS–PAGE, followed by autoradiography. CBB, Coomassie brilliant blue staining; [^{32}P], autoradiography. (**F**) Left panels, constructs used in (**F**, **G**). Right panels, MBP-Dvl2(1–433) or Dvl2(1–433)$^{\Delta 140-263}$ (1.5 μg of each protein) was incubated with GST-Plk1 in kinase reaction buffer, followed by autoradiography. (**G**) MBP-Dvl2(140–358) or Dvl2(140–358)^{T206A} (1.5 μg of each protein) was incubated with GST-Plk1 in kinase reaction buffer, followed by autoradiography.

(Figure 3C; Supplementary Figure S5C). Expression of GFP-mouse (m)Dvl2^{WT}, which is resistant to siRNA against human Dvl2, reduced the spindle angle in Dvl2-depleted cells, but that of GFP-mDvl2^{T206A} did not (Figure 3C). Exogenous GFP-mDvl2^{WT} and GFP-mDvl2^{T206A} in Dvl2-depeleted cells were expressed at two-fold higher levels than endogenous GFP-mDvl2 (Supplementary Figure S6A). GFP-mDvl2^{T206A} localized to the spindles and spindle poles as well as GFP-mDvl2^{WT} (Supplementary Figure S6B and C). These results suggested that the phosphorylation of Dvl2 by Pk1 is necessary for maintaining the correct spindle axis.

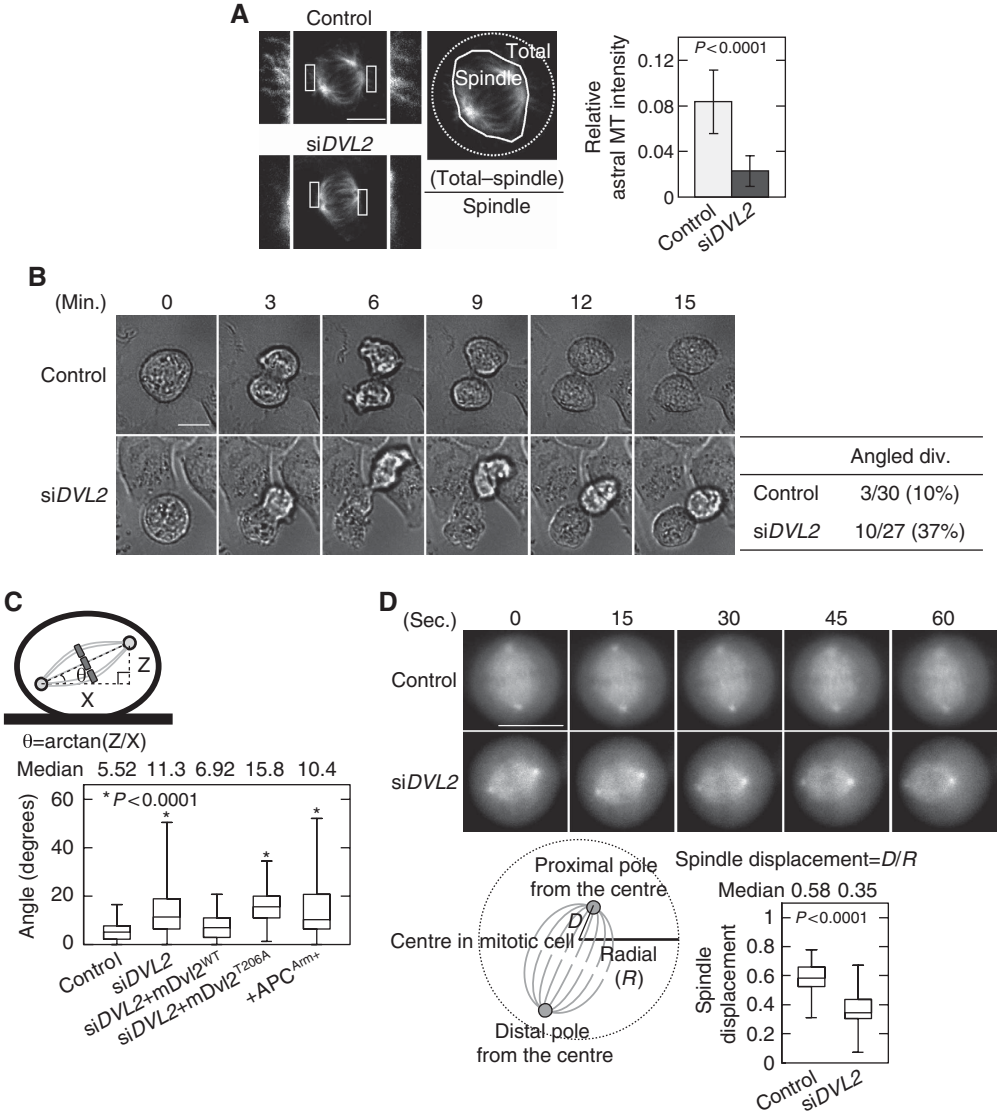

Figure 3 Dvl2 regulates spindle orientation. (**A**) β-Tubulin was stained in control or Dvl2-depleted HeLaS3 cells, and the average relative astral MT intensity was calculated. The intensities of the total MT area and the total spindle area were measured and the relative astral MT intensity is expressed as the ratio of [(intensity of the total MT area)−(intensity of the spindle MT area)]/(intensity of the spindle MT area). Border between astral MT and spindle MT was determined by spindle morphology and intensity threshold. The regions in white boxes are shown enlarged. (**B**) Images of the mitotic control or Dvl2-depleted HeLaS3 cells were acquired every 3 min for 24 h. Mitotic cells were identified from the movie pictures (Supplementary Movies 1 and 2), and then counted as 'plane division' (both daughter cells remained attached to the substratum after cell division) or 'angled division' (one of two daughter cells failed to gain adhesion). (**C**) Top panels, scheme describing spindle angle (θ) measurement. Bottom panels, spindle angles were measured in HeLaS3 cells transfected with the indicated siRNA (si) or plasmids (+). si*DVL2* + mDvl2^{WT} and si*DVL2* + mDvl2^{T206A} indicates Dvl2-depleted HeLaS3 cells expressing GFP-mDvl2^{WT} and GFP-mDvl2^{T206A}, respectively. (**D**) Top panels, for visualizing the spindle in control or Dvl2-depleted cells, HeLa cells stably expressing GFP-EB3 was transfected with each siRNA. At 72 h after transfection, imaging was started. Images of the mitotic control and Dvl2-depleted HeLaS3 cells were acquired every 3 s (Supplementary Movies 3 and 4, respectively). Snap shots are shown at 15 s each. Bottom panels, the radial (*R*) of a metaphase cell and the distance (*D*) from the centre to the proximal spindle pole in a metaphase cell were measured, and spindle displacement was expressed as a ratio of *D* to *R* ($n = 65$). Thirteen cells were captured by time-lapse imaging, and five snap shots were selected at 15 s each from one cell. Scale bars in (**A**), (**B**), and (**D**), 10 μm.

To observe the spindle displacement, living HeLa cells stably expressing GFP-EB3 were used (Ban *et al*, 2009). EB3 is one of an MT plus-end-tracking protein (+TIP) and can be used to visualize the spindles. In control cells, spindles were positioned in the centre of the cell (Figure 3D; Supplementary Movie 3). In contrast, spindles failed to localize to the central position in Dvl2-depleted cells (Figure 3D; Supplementary Movie 4). Taken together, Dvl2 may be required for spindle orientation but not for bipolar spindle formation.

Dvl2 is involved in MT-KT attachment

To know the functions of Dvl2 in the plus-ends of spindle MTs, whether Dvl2 is required for stabilizing MT-KT attachment was examined. EB1 staining was performed after cells were treated with or without a low concentration (12 ng/ml) of nocodazole, which reduces MT dynamics, but does not disrupt bipolar spindle formation (Yasuda *et al*, 2004; Feng *et al*, 2006). As EB1 tends to be concentrated to the MT plus-ends, EB1 staining reveals MT-KT attachment clearly as

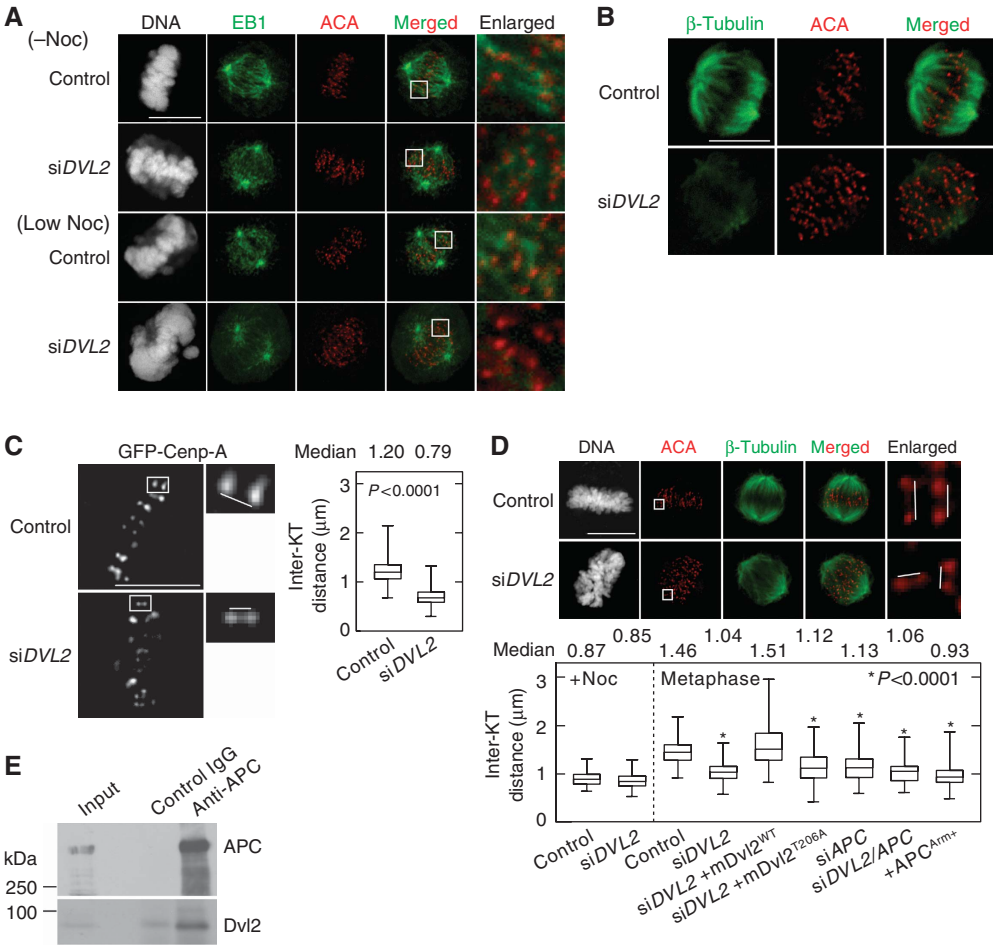

Figure 4 Dvl2 regulates MT-KT attachment. (**A**) Control or Dvl2-depleted HeLaS3 cells were treated with or without a low concentration of nocodazole (12 ng/ml) in the presence of 10 μM MG132 (to arrest cells at metaphase), and the cells were stained with PI (grey), anti-EB1 (green; an MT plus-end marker) antibody, and ACA (red). The regions in white boxes are shown enlarged. (**B**) Control or Dvl2-depleted HeLaS3 cells were treated with a low concentration of nocodazole (12 ng/ml) in the presence of 10 μM MG132 (to arrest cells at metaphase), and the cells were stained with anti-β-tubulin (green) antibody (to observe K-fibres) and ACA (red). (**C**) Control or Dvl2-depleted living HeLa cells expressing GFP-Cenp-A were arrested at metaphase by treatment with 10 μM MG132 for 1 h. Images of cells were captured every 3 s for 3 min. Each KT pair was identified from the movie pictures and the inter-KT distance was measured (control, $n = 627$ KT pairs; si*DVL2*, $n = 586$ KT pairs). (**D**) The inter-KT distance of fixed HeLaS3 cells transfected with the indicated siRNAs (si) or plasmids (+) was measured at metaphase ($n = 100$ KT pairs). Each KT pair was carefully identified from Z-stack images from 0.2 μm-thick sections of a cell. si*DVL2* + mDvl2^{WT} and si*DVL2* + mDvl2^{T206A} indicate Dvl2-depleted HeLaS3 cells expressing GFP-mDvl2^{WT} and GFP-mDvl2^{T206A}, respectively. (**E**) Lysates from mitotic HeLaS3 cells were immunoprecipitated with anti-APC antibody, and immunoprecipitates were probed with anti-APC and anti-Dvl2 antibody. Scale bars in (**A**), (**B**), and (**C**), 10 μm.

compared with MTs stained with anti-β-tubulin antibody. EB1 is also known to be a representative marker for the rate of MT nucleation activity (Piehl *et al*, 2004). Plus-ends of spindle MTs were associated with the centromeres (ACA staining) on metaphase chromosomes in control HeLaS3 cells (Figure 4A). The low concentration of nocodazole induced chromosome misalignment, but MT-KT attachment was not affected in control cells (Figure 4A). Chromosomes were misaligned on the metaphase plate with a failure of chromosome congression in Dvl2-depleted cells (Figure 4A). In these cells, EB1 signals at the plus-ends of spindle MTs were slightly reduced, but still associated with KTs. Depletion of Dvl2 enhanced a failure of chromosome congression and caused the dissociation of MTs from KTs in nocodazole-treated cells (Figure 4A).

We also observed MTs using an anti-β-tubulin antibody in the presence of a low concentration of nocodazole, because mature MT-KT attachments stabilize MTs called kinetochore-fibres (K-fibres) (Sillje *et al*, 2006). K-fibres disappeared in Dvl2-depleted cells treated with a low concentration of nocodazole, whereas K-fibres in control cells were resistant to reduction of spindle dynamics by nocodazole treatment (Figure 4B). However, depletion of Dvl2 alone did not affect the amount of spindle MTs (by assessment of β-tubulin staining), spindle pole distance (by assessment of γ-tubulin staining when measuring the spindle angle), and MT nucleation activity (by assessment of EB1 staining) (Supplementary Figure S7). These results suggested that Dvl2 is required for generating stable MT-KT attachment rather than regulating the stabilization of MTs themselves in mitosis.

It is known that insufficient attachment for both MT-KT and astral MTs to the cell cortex causes a reduction in the pulling force from spindle MTs on KTs at metaphase (Draviam *et al*, 2006; McCartney and Näthke, 2008). To quantitate the inter-KT tension, the inter-KT distance was

measured in live HeLa cells stably expressing GFP-Cenp-A (Uchida *et al*, 2009) (Figure 4C). In control HeLa cells, the inter-KT distance between sister KTs was 1.20 μm at metaphase (Figure 4C; Supplementary Movie 5). By depleting Dvl2, the inter-KT distance in metaphase chromosomes decreased to 0.79 μm (Figure 4C; Supplementary Movie 6). Similar observations were confirmed in fixed HeLaS3 cells (Figure 4D). In addition, ectopic expression of GFP-mDvl2^{WT} in Dvl2-depleted HeLaS3 cells elongated the distance to the same level as control cells, but that of Dvl2^{T206A} did not (Figure 4D). These results suggested that Plk1-dependent phosphorylation of Dvl2 is required for the regulation of the effect on inter-KT distance.

The + TIPs mediate both the interaction of astral MTs with the cell cortex and spindle MTs with KTs (Akhmanova and Hoogenraad, 2005). APC, which functions as a component in the Wnt signalling pathway, is a + TIP and also regulates dynamics of MT plus-ends (McCartney and Näthke, 2008). Consistent with previous observations, depletion of APC reduced the inter-KT distance (Figure 4D; Supplementary Figure S8). Phenotypic similarities between the depletion of Dvl2 and APC suggested that both proteins interact functionally in mitosis. An interaction between Dvl and APC was indeed observed in mitotic HeLaS3 cells (Figure 4E), and expression of the armadillo domain of APC (APC^{Arm+}), which binds to endogenous Dvl and inhibits the binding of Dvl2 and APC (Matsumoto *et al*, 2010), increased the spindle angle (Figure 3C) and reduced the inter-KT distance (Figure 4D). Taken together, the binding of Dvl2 to APC might regulate the dynamics of MT plus-ends cooperatively with APC in mitosis.

Dvl2 is required for SAC activation through Mps1 activation

The cell population at prometaphase in mitosis was higher in Dvl2-depleted cells than in control cells (Supplementary Figure S9), whereas the mitotic index was not changed by the depletion of Dvl2 in HeLaS3 cells (Figure 5A). The SAC ensures the accuracy of chromosome segregation during mitosis, and components of the SAC accumulate at KTs after treatment with MT poisons. As GFP-Dvl2 accumulated at the KTs after treatment with nocodazole (see Figure 1C), we examined whether Dvl2 functions in SAC. Depletion of Dvl2 reduced the numbers of mitotic cells increased by the treatment with nocodazole or taxol, which induce mitotic arrest if the SAC is intact (Figure 5A). Expression of GFP-mDvl2^{WT} increased the mitotic index that was reduced in nocodazole-treated Dvl2-depleted HeLaS3 cells (Figure 5A). GFP-mDvl2^{T206A} could also rescue the phenotype in Dvl2-depleted cells (Figure 5A), and GFP-mDvl2^{T206A} localized to the KTs when cells were treated with nocodazole as well as GFP-mDvl2^{WT} (Supplementary Figure S10A). The similar findings were observed in U2OS cells (Supplementary Figure S10B). These results suggested that Dvl2 is required for activation of the SAC in a Plk1-phosphorylation-independent manner. Therefore, it is likely that Plk1-mediated phosphorylation of Dvl2 is required for proper spindle positioning and MT-KT attachment, but not for the SAC.

Mps1 is a KT-associated kinase, and autophosphorylation-dependent activation of Mps1 is required for SAC (Abrieu *et al*, 2001; Stucke *et al*, 2002; Liu *et al*, 2003; Vigneron *et al*, 2004; Kang *et al*, 2007; Jelluma *et al*, 2008a). Depletion of Dvl2 reduced mitotic autophosphorylation of Mps1 (the upper band of Mps1) (Figure 5B). Consistent with this finding, the activation of Mps1 monitored by the phosphorylation of Cenp-A at serine 7 (Jelluma *et al*, 2008b) was also decreased in Dvl2-depleted cells (Figure 5C). Depletion of BubR1 did not decrease the level of phosphorylated Mps1, rather slightly increased the total amount of Mps1 (the sum of upper and lower bands of Mps1) (Figure 5B; Supplementary Figure S11A). Therefore, it is likely that Mps1 acts downstream of Dvl2 and independent of or in parallel with BubR1.

The presence of SAC kinases Bub1 and BubR1 at the KTs was suggested to be necessary for the SAC (Taylor and McKeon, 1997; Cleveland *et al*, 2003; Kiyomitsu *et al*, 2007; Musacchio and Salmon, 2007). Although depletion of Dvl2 did not affect the protein levels of Bub1 or BubR1 (Supplementary Figures S11B and S14A), their localization to the KTs was reduced in Dvl2-depleted cells even after SAC activation by nocodazole treatment (Figure 5D). Expression of GFP-mDvl2^{WT} rescued this phenotype (Figure 5D; Supplementary Figure S11C). As Hec1, an outer KT molecule, was colocalized with ACA in Dvl2-depleted cells (Supplementary Figure S11D), it is conceivable that depletion of Dvl2 did not affect the KT structure that provides a landing platform for SAC proteins. Therefore, Dvl2 may be required for the recruitment of Bub1 and BubR1 to the KTs.

Although Dvl2 formed a complex with Mps1 at endogenous levels in asynchronous HeLaS3 cells, the complex dissociated in mitosis (Figure 5E), suggesting that the binding itself may not be necessary for the activation of Mps1. Dvl2 did not form a complex with BubR1 in mitosis (Supplementary Figure S11E). Under the same conditions, APC did not interact with Mps1 (Supplementary Figure S11F). Taken together, Dvl2 appears to be involved in the activation of Mps1 and the localization of Bub1 and BubR1 to KTs, but it is unlikely that Dvl2 functions as a scaffold protein to recruit Mps1, Bub1, or BubR1.

LRP6 and Fz2 have a function in spindle orientation

Finally, it was examined whether Wnts and their receptors are involved in Dvl2-mediated mitotic functions (Figure 6A). Consistent with the previous report (Davidson *et al*, 2009), the phosphorylation of LRP6 at S1490, through cyclin Y/Pftk, was increased in mitosis (Figure 6B; Supplementary Figure S12A). This phosphorylation is also known to be induced by the stimulation of certain Wnts, such as Wnt3a (MacDonald *et al*, 2009; Sakane *et al*, 2010; Sato *et al*, 2010). Another Wnt receptor Fz2 has been shown to have a function in both the β-catenin-dependent and -independent pathways in HeLaS3 cells (Sato *et al*, 2010). Depletion of Fz2 or Dvl2 repressed the phosphorylation of LRP6 at Ser1490 in mitosis (Figure 6B and C), suggesting that the mitotic phosphorylation of LRP6 at S1490 is dependent on Fz2 and Dvl2. Although Dkk1 did not affect the phosphorylation of LRP6 at Ser1490 (Supplementary Figure S12B), whether a Wnt ligand is involved in the phosphorylation of LRP6 is not known at present (see Discussion). Depletion of Fz2 or LRP6 did not affect mitotic phosphorylation of Dvl2 (Supplementary Figure S12C), suggesting that the phosphorylation of Dvl2 in mitosis does not require these Wnt receptors.

To clarify the function of LRP6 and Fz2 in mitosis, the spindle rotation in LRP6- or Fz2-depleted cells was examined. Depletion of LRP6 or Fz2 increased the spindle angle,

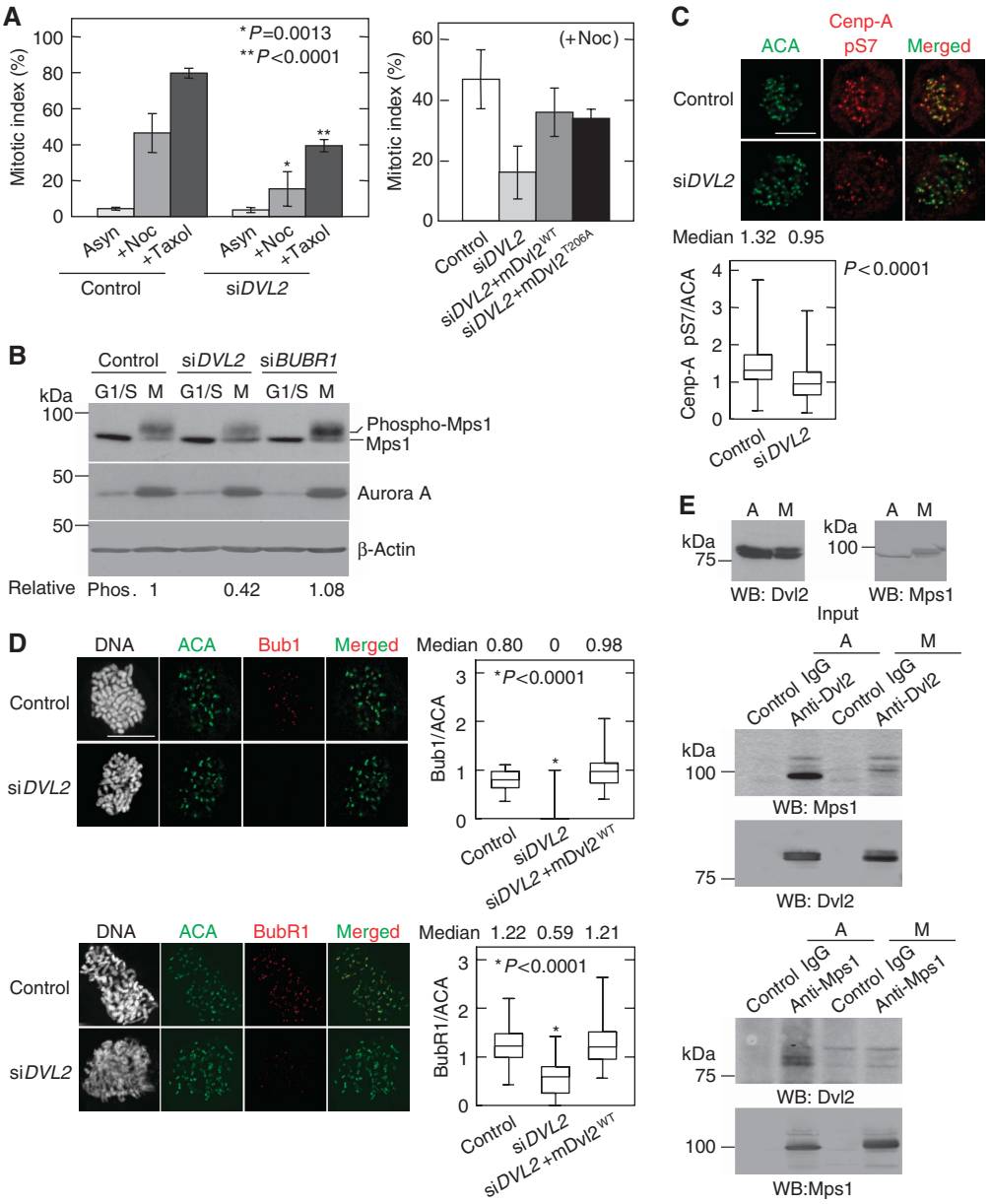

Figure 5 Dvl2 is involved in the SAC. (**A**) Left panel, control or Dvl2-depleted HeLaS3 cells were treated with 100 ng/ml nocodazole or 10 nM taxol for 24 h and then stained with an anti-MPM2 antibody and PI. The ratios of mitotic cells (mitotic index) among >100 cells were calculated. Right panel, GFP-mDvl2^{WT} or GFP-mDvl2^{T206A} was expressed in Dvl2-depleted HeLaS3 cells treated with 100 ng/ml nocodazole, and the mitotic index was calculated after nocodazole treatment. (**B**) Control or Dvl2-depleted HeLaS3 cells were synchronized as shown in Supplementary Figure S2B. Lysates from G1/S phase (G1/S) or mitotic phase (M) cells were probed with the indicated antibodies. β-Actin was used as a loading control. (**C**) Control or Dvl2-depeleted HeLaS3 cells were treated with 10 μM MG132 for 2 h, and then the cells were stained for ACA (green) and phospho-Ser7 of Cenp-A (red). The peaked intensities of Cenp-A pS7 and ACA were measured at each KT, and the ratio of the intensity of Cenp-A pS7 to ACA was calculated (control, $n=141$ KT pairs; si*DVL2*, $n=240$ KT pairs). (**D**) Control cells, Dvl2-depleted HeLaS3 cells, or Dvl2-depleted HeLaS3 cells expressing GFP-mDvl2 were treated with 200 ng/ml nocodazole for 1 h to activate SAC. After antibody reactions, DNA was stained with PI, and then mitotic cells were identified by condensed DNA. Peaked intensity of Bub1, BubR1, and ACA was measured at each KT in mitotic cells, and the ratio of the intensity of BubR1 or Bub1 to ACA was calculated ($n=100$ KT pairs). (**E**) Lysates from asynchronous (A) and thymidine-nocodazole blocked (M) HeLaS3 cells were immunoprecipitated with the indicated antibodies, and the immunoprecipitates were probed with anti-Dvl2 and anti-Mps1 antibodies. Scale bar in (**C**) and (**D**), 10 μm.

whereas that of another Wnt receptor Ror2 or Wnt5a did not affect the spindle angle (Figure 6D). Soluble Fz-related protein2 (sFRP2) interacts with Wnts, thereby inhibiting Wnt signalling (Kawano and Kypta, 2003). Overexpression of Dkk1 or addition of sFRP2-conditioned medium (CM) increased the spindle angle (Figure 6D and E). Furthermore, fibres of astral MTs were reduced in LRP6- or Fz2-depleted cells as well as Dvl2-depleted cells (Figure 6F). Taken together, LRP6 and Fz2 are involved in the regulation of proper spindle axis. These Wnt receptors are thought to activate the β-catenin pathway (Kikuchi *et al*, 2009; MacDonald *et al*, 2009). However, ectopic expression of a dominant-negative Tcf4 (TcfDN) (Tetsu and McCormick, 1999) did not affect spindle axis (Figure 6D), suggesting that gene expression induced by β-catenin and Tcf/Lef is not required for spindle orientation. Therefore, a novel

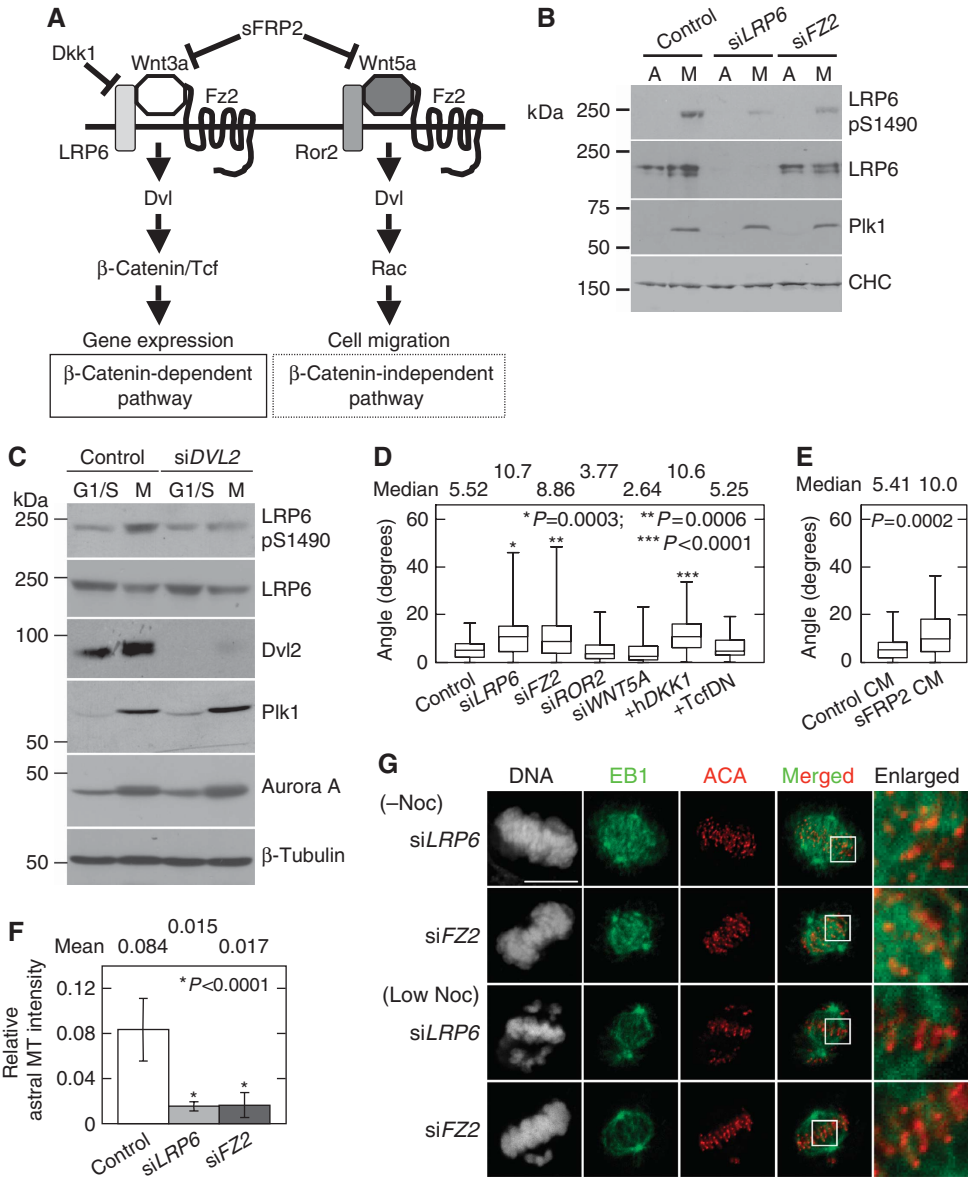

Figure 6 Wnt receptors are involved in spindle orientation, but not in MT-KT attachment. (**A**) Outline of the Wnt signalling pathway. (**B**) Mitotic cells of control, LRP6-depleted, or Fz2-depleted HeLaS3 cells were collected by mechanical shake-off after nocodazole treatment, and then lysates from asynchronous (A) or mitotic cells (M) were probed with the indicated antibodies. CHC was used as a loading control. (**C**) Control or Dvl2-depleted HeLaS3 cells were synchronized as in Supplementary Figure S2B. Lysates from G1/S phase (G1/S) and mitotic phase (M) cells were probed with the indicated antibodies. β-Tubulin was used as a loading control. (**D**) The spindle axis of HeLaS3 cells transfected with the indicated siRNAs (si) or plasmids (+) was measured as described in Figure 3C. (**E**) After HeLaS3 cells were treated with control or sFRP2-conditioned medium (CM) for 22 h, the cells were arrested at metaphase by treatment with 10 μM MG132 for 2 h. Then, the spindle axis of the cells was measured. (**F**) The average relative astral MT intensity in LRP6-depleted or Fz2-depleted cells was calculated. (**G**) LRP6 or Fz2-depleted HeLaS3 cells were treated with or without a low concentration of nocodazole (12 ng/ml) in the presence of 10 μM MG132 and then stained for EB1, centromere (ACA), or DNA (PI). Scale bars in (**G**), 10 μm.

signalling pathway through LRP6, Fz2, and Dvl2 may be involved in spindle orientation.

It was examined whether LRP6 and Fz2 are required for MT-KT attachment. Depletion of LRP6 or Fz2 caused the failure of chromosome congression at metaphase, but did not abolish MT-KT attachment in the absence of nocodazole (Figure 6G). Depletion of LRP6 or Fz2 enhanced the failure of chromosomal congression in the cells treated with a low concentration of nocodazole, and the percentage of cells with misaligned chromosomes increased from 79 to 86% (Figure 6G; Supplementary Figure S13A). However, it did not affect MT-KT attachment (Figure 6G). K-fibres were resistant to reduction of spindle dynamics by the treatment with a low concentration of nocodazole in LRP6- or Fz2-depleted cells (Supplementary Figure S13B). These results suggest that chromosome misalignment by depletion of Fz2 or LRP6 is not due to the failure in MT-KT attachment. Depletion of LRP6 or Fz2 did not affect mitotic accumulation of Plk1 (Figure 6B). Furthermore, depletion of LRP6 or Fz2 did not affect the SAC, because the number of mitotic cells increased after nocodazole treatment in LRP6- or Fz2-depleted cells as well as control cells (data not shown).

Discussion

This study showed that depletion of Dvl2 causes spindle misorientation and reduces the inter-KT distance. Insufficient MT-KT attachment was also observed in Dvl2-depleted cells. In addition, Dvl2 was required for SAC activation. These results suggest that Dvl2 has functions in mitotic progression.

There are three homologues of the Dvl family in mammals (Wharton, 2003). HeLaS3 cells expressed three Dvls, Dvl1, Dvl2, and Dvl3 (Supplementary Figure S14A). Depletion of either Dvl1, Dvl2, or Dvl3 alone generated abnormalities in the spindle axis (Supplementary Figure S14B) and the failure of SAC activation (Supplementary Figure S14C), and the extent of the phenotypes by depletion of all of Dvl1, Dvl2, and Dvl3 was similar to that by the depletion of Dvl2 alone (Supplementary Figure S14B and C). As the efficiency of the depletion of each Dvl was >90% (Supplementary Figure S14A), it is conceivable that Dvls do not act on these mitotic functions redundantly. Dvls may function as a heterotrimer, because it was shown that Wnt3a-dependent transcription was suppressed by depletion of either of Dvl1, Dvl2, or Dvl3 and that Dvl1 and Dvl3 are found in a Dvl2 immunoprecipitation (Lee *et al*, 2008). Therefore, the cells in which Dvl2 was depleted were used in this study.

Impact of Dvl2 on spindle orientation, MT-KT attachment, and SAC activation

Spindle misorientation may be caused by insufficient attachment of the astral MT plus-end to the cell cortex, because depletion of +TIPs, such as EB1 and APC, or cortical factors, such as Myosin X and β_1-integrin, has been reported to cause spindle misorientation (Draviam *et al*, 2006; Toyoshima and Nishida, 2007). Therefore, Dvl2 may be involved in the attachment of the astral MT plus-end to the cell cortex. The dynamics of MT plus-ends are also essential for the establishment of MT-KT attachment (Akhmanova and Hoogenraad, 2005; Tanaka *et al*, 2005). Plk1 is known to phosphorylate KT components including BubR1 and regulates the establishment of MT-KT attachment (Elowe *et al*, 2007; Matsumura *et al*, 2007). Our results showed that depletion of Dvl2 suppresses the recruitment of Bub1 and BubR1 to the KTs. As the loss of these proteins at the KTs affects MT-KT attachment (Lampson and Kapoor, 2005; Meraldi and Sorger, 2005), it is also possible that the phenotypes in Dvl2-depleted cells might be due to the failure in the constitution of the KTs. Dvl2 was found to be a substrate of Plk1 in mitosis, and T206 of Dvl2 was identified as a phosphorylation site. Ectopic expression of $Dvl2^{T206A}$ could not rescue the abnormal spindle angle and inter-KT distance in Dvl2-depleted HeLaS3 cells, suggesting that the phosphorylation of Dvl2 by Plk1 is necessary for the proper spindle positioning and MT-KT attachment through regulating the dynamics of MT plus-ends.

How does Dvl2 regulate the dynamics of MT plus-ends in mitosis? APC is known to regulate the stability of MTs by binding to them (McCartney and Näthke, 2008). It has been shown that Dvl2 forms a complex with APC and is involved in the dynamics of MT plus-ends in interphase (Matsumoto *et al*, 2010). The interaction between APC and Dvl2 was confirmed in mitosis in this study. In addition, the inhibition of APC and Dvl2 because of the expression of APC^{Arm+} disturbed the spindle angle and the inter-KT distance. Therefore, if Dvl localized to the cell cortex or KTs associates with APC at the plus-end of mitotic spindles and the biding of both proteins are necessary for the stabilization of spindles, Dvl2 may regulate the dynamics of MT plus-ends cooperatively through the interaction with APC. The spindle pole distance and the intensity of the spindle staining with an anti-β-tubulin antibody in Dvl2-depeleted cells were similar to those in control cells. These results support that Dvl2 is involved in the dynamics of MT plus-ends rather than in the stabilization of MTs themselves.

The SAC monitors the interaction between KTs and spindle MTs. This study showed that the SAC is only partially active in Dvl2-depleted cells. Mps1 is an important player in that it is required for the localization of other SAC kinases to the KTs in *Xenopus* (Abrieu *et al*, 2001; Vigneron *et al*, 2004). However, there are different arguments in this activity of Mps1 in human cells (Liu *et al*, 2003; Kang *et al*, 2007). The present results showed that the depletion of Dvl2 decreases Mps1 activity. Dvl2 was found to form a complex with Mps1 in the interphase, whereas this complex dissociated in mitosis. Therefore, the binding to Dvl2 may not be necessary for the activation of Mps1 in mitosis. However, how Dvl2 is involved in the regulation of Mps1 is not known at present.

It has been shown that KT localization of Bub1 and Blinkin-dependent KT localization of BubR1 are required for the SAC (Taylor and McKeon, 1997; Kiyomitsu *et al*, 2007). Taken together with observations that Dvl2 is required for the KT localization of Bub1 and BubR1, Dvl2 appears to be involved in the activation of Mps1, and Dvl2 dissociated from Mps1 may attach to the KTs and be involved in the recruitment of Bub1 and BubR1 to the KTs. $Dvl2^{T206A}$ could rescue an SAC defect as well as $Dvl2^{WT}$ (see Figure 5A), suggesting that Plk1-dependent phosphorylation of Dvl2 is dispensable for SAC activation. Indeed, the SAC was previously shown to be active in Plk1-depleted cells, with checkpoint proteins still associated with KTs (Sumara *et al*, 2004; van Vugt *et al*, 2004; Elowe *et al*, 2007; Lénárt *et al*, 2007; Santamaria *et al*, 2007). Therefore, Dvl2 has two distinct mitotic functions, the regulation of proper spindle positioning and MT-KT attachment in a Plk1-dependent manner and the SAC in a Plk1-independent manner.

Wnt signalling and mitosis

It has been shown that LRP6 is phosphorylated at Ser1490 by the mitotic cyclin Y and Pftk complex and thereby the β-catenin-dependent pathway is active and effective in mitosis (Davidson *et al*, 2009). However, how Wnt signalling is involved in the regulation of mitotic progression is not clear at the moment. Wnt activates β-catenin-dependent and independent pathways and Dvl mediates both pathways (Wharton, 2003; Kikuchi *et al*, 2009). It is unlikely that the β-catenin-independent pathway is involved in the functions of Dvl in spindle orientation, because depletion of Wnt5a and Ror2, which are a representative ligand and receptor that activate the β-catenin-independent pathway (Green *et al*, 2008; Kikuchi *et al*, 2009), did not affect the spindle axis.

LRP6, Fz2, and Dkk1 were involved in the regulation of the spindle axis. Although these molecules are known to regulate the β-catenin-dependent pathway, a dominant-negative form of Tcf4 did not affect the spindle axis, suggesting that there may be a novel pathway through LRP6-Fz2-Dvl2 to regulate the spindle axis beyond transcriptional activation. GSK3β and

β-catenin act downstream of Dvl; however, whether the novel pathway is linked to these molecules in mitosis is not known at present. As depletion of LRP6 or Fz2 did not affect MT-KT attachment or mitotic index in the presence of nocodazole, this pathway could not be involved in the SAC.

Dkk1 did not affect mitotic phosphorylation of Dvl2. Consistent with this finding, depletion of LRP6 or Fz2 did not affect mitotic phosphorylation of Dvl2. Therefore, it is intriguing to speculate that mitotic phosphorylation of Dvl2 is dependent on Plk1, but independent of Wnt signalling. However, because the phosphorylation of Dvl was assessed using a mobility shift on an SDS-gel, we cannot exclude the possibility that Wnt induces the phosphorylation of Dvl, which is not indicated as a mobility shift. Although Dkk1 inhibits GSK3- or casein kinase Iγ-mediated LRP6 phoshorylation at Ser1490 or Thr1479 in response to Wnt3a in interphase cells (Sakane *et al*, 2010), Dkk1 did not affect LRP6 phosphorylation at Ser1490, but inhibited the phosphorylation at Thr1479 slightly in mitosis (see Supplementary Figure S12B). As Ser1490 of LRP6 is phosphorylated by cyclin Y/Pftk1 in mitosis (Davidson *et al*, 2009), the reason for the failure of Dkk1 to inhibit the LRP6 phosphorylation might be due to that Ser1490 of LRP6 is phosphorylated by cyclin Y/Pftk more dominantly than a Wnt signal. However, it is still possible that Wnt-dependent phosphorylation of LRP6 is inhibited by Dkk1 in mitosis, because LRP6 is phosphorylated at other threonine and serine residues (Davidson *et al*, 2005; MacDonald *et al*, 2009).

Here, we showed that Dvl2 is involved in the regulation of faithful mitotic progression through the following mechanisms (Figure 7). First, appropriate spindle orientation regulated by Dvl2 depends on Plk1-dependent phosphorylation of Dvl2 and Wnt receptor-mediated novel signalling. Second, MT-KT attachment regulated by Dvl2 requires Plk1-dependent phosphorylation of Dvl2, but not Wnt receptors. Last, SAC activation by Dvl2 is independent of both Plk1 and Wnt receptors. The present results provide a new concept that Dvl2 is a regulator for faithful mitotic progression.

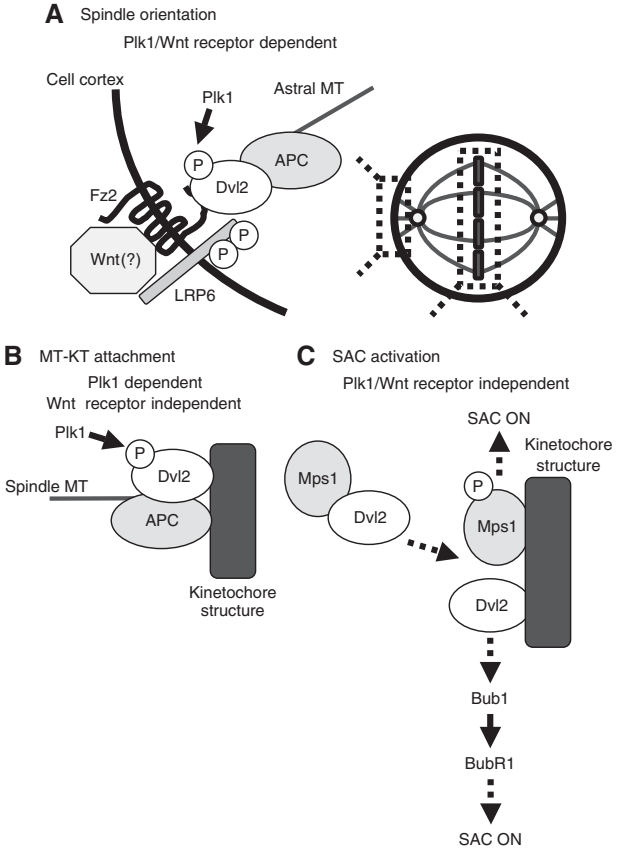

Figure 7 Possible model for mitotic functions of Dvl2. (**A**) Spindle orientation regulated by Dvl2 depends on Plk1-dependent phosphorylation of Dvl2 and on Wnt receptors. (**B**) MT-KT attachment regulated by Dvl2 requires Plk1-dependent phosphorylation of Dvl2, but not Wnt receptors. (**C**) SAC activation by Dvl2 is independent of both Plk1 and Wnt receptors.

Materials and methods

Reagents and antibodies

HeLa cells stably expressing GFP-EB3 or GFP-Cenp-A were provided by K Urano and T Hirota (Ban *et al*, 2009; Uchida *et al*, 2009). CM containing sFRP2 was prepared and Dkk1-FLAG was purified from CM as described previously (Kurayoshi *et al*, 2006; Sakane *et al*, 2010). MG132, nocodazole, paclitaxel, thymidine, fibronectin, and poly-L-lysine were from Calbiochem and Sigma-Aldrich. All of the primary antibodies used in this study are listed in Supplementary Table S1. Secondary antibodies coupled to horse radish peroxidase were purchased from Jackson ImmunoResearch Laboratories. Secondary antibodies coupled to AP were purchased from Promega. Secondary antibodies used for immunofluorescence were from Molecular Probes. All of the siRNAs used in this study are listed in Supplementary Table S2.

Cell culture, synchronization, and transfection

HeLaS3 or U2OS cells were maintained in DMEM supplemented with 10% FBS and penicillin-streptomycin. For cell staining and image analysis, cells were seeded on fibronectin- or poly-L-lysine-coated coverslips. HEK293 cells were maintained in DH10 medium supplemented with 10% FBS and penicillin-streptomycin. Methods for plasmid transfection and siRNA were described previously (Niikura *et al*, 2006). Synchronization of cells was performed by treatment with 100 ng/ml nocodazole for 16 h (Figure 2A–D) or 10 μM MG132 for 2 h (Figures 3A, C, 4D, 5C, 6D–F; Supplementary Figures S5C, S7A, and S7B). For the thymidine-nocodazole block (Figures 4E, 5E and 6B; Supplementary Figures S2A, S11E, S11F, and S12C), HeLaS3 cells at 40% confluency were washed twice with phosphate-buffered saline (PBS), and medium containing 2 mM thymidine was added for 24 h (G1/S phase block). After the thymidine block, thymidine was removed by washing three times with PBS, and fresh medium was added for 3 h to release the cells. After the cells were released from the thymidine block, 100 ng/ml nocodazole was added into the medium for 12 h (mitotic block). After the nocodazole block, mitotic cells were collected by mechanical shake-off, nocodazole was removed by washing three times with PBS, and fresh medium was added to release the cells. For the double-thymidine-MG132 block (Figures 5B and 6C; Supplementary Figures S2C, S11A, S11B, and S12B), HeLaS3 cells at 25–30% confluency were washed twice with PBS, and medium containing 2 mM thymidine was added for 18 h (first block). After the first thymidine block, thymidine was removed by washing three times with PBS, and fresh medium was added for 9 h to release the cells. Then, medium containing 2 mM thymidine was added for 17 h (second block). After the second block, thymidine was removed by washing three times with PBS, and the cells were released by adding fresh medium. Then, the cells were arrested at metaphase by treatment with 10 μM MG132 for 2 h at 7.5 h after release from a double-thymidine block. After the MG132 block, mitotic cells were collected by mechanical shake-off.

Cell staining and image analysis

Methods for immunofluorescence were described previously (Niikura *et al*, 2006; Toyoshima and Nishida, 2007). For staining of GFP-Dvl2, U2OS or HeLaS3 cells expressing GFP-Dvl2 were fixed with 100% methanol for 30 min at −20°C. The cells were washed three times with PBS, and blocked for 20 min with 1% BSA in PBS including 0.05% Tween-20 (PBST). The cells were then incubated

with anti-GFP and other antibodies for 2 h at room temperature (RT) or overnight at 4°C. After the cells were washed three times with PBS, they were incubated with the fluorescent secondary antibodies, Alexa Fluor 488, Alexa Fluor 546, or Alexa Fluor 633 (Invitrogen) for 1 h at RT. Coverslips were washed extensively with PBS and then mounted in 50% glycerol containing propidium iodide (PI) (Wako, Japan) and RNase A (Sigma-Aldrich) to stain the DNA. All processing and measurements were carried out using an LSM510 system with Axiovision (Carl Zeiss, Germany), except for time-lapse images. For time-lapse imaging, we used an inverted microscope (IX81; Olympus, Japan). Supplementary Movies 3–6 were captured every 3 s for 3 min, and Supplementary Movies 1 and 2 were captured every 3 min for 24 h (Supplementary Movies 1–6 were started at 72 h after siRNA transfection). Images were treated with MetaMorph software (MDS Analytic Technologies) and ImageJ (National Institutes of Health).

Measurement of spindle axis

Coverslips coated with fibronectin were used. For double staining of β-tubulin and γ-tubulin, cells were fixed with 100% methanol for 30 min at −20°C. Cells were washed twice with PBS and blocked for 20 min with 1% BSA in PBST. Cells were stained with mouse anti-β-tubulin and rabbit anti-γ-tubulin antibodies (Sigma). After the primary antibody reaction, the cells were counterstained with Alexa Fluor633-goat anti-mouse and Alexa Fluor488-goat anti-rabbit IgG antibodies (Molecular Probes). DNA was stained using PI/RNase treatment. On the basis of γ-tubulin intensity, the linear distance and the vertical distance between the two poles of the metaphase spindles were measured by taking Z-stack images from 0.2 μm-thick sections of a metaphase cell. The spindle angle between the axis of a metaphase spindle and that of substrate surface was calculated with an inverse trigonometric function. All processing and measurements were carried out using an LSM510 system with Axiovision.

Measurement of spindle displacement

For visualizing the spindles in control or Dvl2-depleted cells, HeLa cells stably expressing GFP-EB3 was transfected with each siRNA, and at 72 h after transfection, imaging was started in the presence of 10 μM MG132 to arrest the cells at metaphase. Images of the mitotic control or Dvl2-depleted HeLaS3 cells were acquired every 3 s for 3 min. Radial (*R*) of a metaphase cell and distance (*D*) from the centre to the proximal spindle pole in a metaphase cell were measured and spindle displacement was expressed as a ratio of *D* to *R*.

Measurement of astral MT intensity

Coverslips coated with fibronectin were used. The methods for cell fixation and β-tubulin staining were described previously (Thoma *et al*, 2009). Cells were pre-extracted with PHEM buffer (60 mM Pipes-NaOH at pH 6.9, 25 mM Hepes-NaOH at pH 6.9, 10 mM EGTA, and 4 mM $MgSO_4$) including 0.5% Triton X-100 and 5 μM fresh taxol for 1 min, and then fixed for 5 min with cold methanol at −20°C before staining with an anti-β-tubulin antibody. Relative astral MT intensity was calculated by the following equation: relative astral MT intensity = [(intensity of the total MTs area) − (intensity of the spindle MT area)]/(intensity of the spindle MT area) (Thoma *et al*, 2009). All processing and measurements were carried out using an LSM510 system with Axiovision.

Measurement of MT-KT attachment

Cells were treated with both 12 ng/ml nocodazole and 10 μM MG132 for 2 h and then fixed with 100% methanol for 30 min at −20°C. Cells were stained with mouse anti-EB1 antibody and human ACA or mouse anti-β-tubulin antibody and human ACA. After the primary antibody reaction, cells were counterstained with Alexa Fluor633-goat anti-mouse and Alexa Fluor488-goat anti-rabbit IgG antibodies (Molecular Probes). DNA was stained using PI/RNase treatment. All processing and measurements were carried out using LSM510 system with Axiovision.

Measurement of inter-KT distance

For the measurement of inter-KT distance using HeLa cells expressing GFP-Cenp-A, cells were arrested at metaphase by treatment with 10 μM MG132 for 1 h (Figure 4C). Cells were captured every 3 s for 3 min using an inverted microscope (IX81; Olympus). Data analysis was performed using ImageJ (NIH), and each KT pair was identified using movie pictures.

For the measurement of inter-KT distance in fixed cells, cells were arrested at metaphase by treatment with 10 μM MG132 for 2 h (Figure 4D) and then fixed with 100% methanol for 30 min at −20°C. Cells were washed twice with PBS and blocked for 20 min with 1% BSA in PBST. Cells were stained with mouse anti-β-tubulin antibody and ACA. After the primary antibody reaction, the cells were counterstained with Alexa Fluor633-goat anti-mouse and Alexa Fluor488-goat anti-human IgG antibodies. DNA was stained using PI/RNase treatment. Each KT pair was identified carefully from Z-stack images from 0.2 μm-thick sections of a cell.

Statistics

The experiments were performed at least four times and the results were expressed as means ± s.e. or median ± s.d. of at least four independent experiments. Statistical analysis was performed using StatView-J 5.0 software (SAS Institute Inc). Differences between the data were tested for statistical significance using *t*-test. *P*-values <0.01 were considered statistically significant.

Supplementary data

Supplementary data are available at *The EMBO Journal* Online (http://www.embojournal.org).

Acknowledgements

We thank E Nishida, S Matsuura, T Yamamoto, M Bornens, K Urano, T Hirota, and Y Mimori-Kiyosue for donating plasmids, antibodies, and cell lines, and S Sadakane for technical assistance. We also thank Drs H Saya, T Hirota, and laboratory members for helpful discussion. Financial support was provided by Grants-in-Aid for Scientific Research and for Scientific Research on Priority Areas from the Ministry of Education, Science, and Culture of Japan (2007, 2008, 2009), and by Research Grants from the Princess Takamatsu Cancer Research Fund (08-24005) and Takeda Science Foundation (2009).

Conflict of interest

The authors declare that they have no conflict of interest.

References

Abrieu A, Magnaghi-Jaulin L, Kahana JA, Peter M, Castro A, Vigneron S, Lorca T, Cleveland DW, Labbe JC (2001) Mps1 is a kinetochore-associated kinase essential for the vertebrate mitotic checkpoint. *Cell* **106:** 83–93

Akhmanova A, Hoogenraad CC (2005) Microtubule plus-end-tracking proteins: mechanisms and functions. *Curr Opin Cell Biol* **17:** 47–54

Andersen SS (2000) Spindle assembly and the art of regulating microtubule dynamics by MAPs and Stathmin/Op18. *Trends Cell Biol* **10:** 261–267

Arnaud L, Pines J, Nigg EA (1998) GFP tagging reveals human Polo-like kinase 1 at the kinetochore/centromere region of mitotic chromosomes. *Chromosoma* **107:** 424–429

Bahmanyar S, Kaplan DD, Deluca JG, Giddings Jr TH, O'Toole ET, Winey M, Salmon ED, Casey PJ, Nelson WJ, Barth AI (2008) β-Catenin is a Nek2 substrate involved in centrosome separation. *Genes Dev* **22:** 91–105

Ban R, Matsuzaki H, Akashi T, Sakashita G, Taniguchi H, Park SY, Tanaka H, Furukawa K, Urano T (2009) Mitotic regulation of the stability of microtubule plus-end tracking protein EB3 by ubiquitin ligase SIAH-1 and Aurora mitotic kinases. *J Biol Chem* **284:** 28367–28381

Casenghi M, Meraldi P, Weinhart U, Duncan PI, Korner R, Nigg EA (2003) Polo-like kinase 1 regulates Nlp, a centrosome protein involved in microtubule nucleation. *Dev Cell* **5:** 113–125

Ciani L, Krylova O, Smalley MJ, Dale TC, Salinas PC (2004) A divergent canonical WNT-signaling pathway regulates microtubule dynamics: dishevelled signals locally to stabilize microtubules. *J Cell Biol* **164:** 243–253

Cleveland DW, Mao Y, Sullivan KF (2003) Centromeres and kinetochores: from epigenetics to mitotic checkpoint signaling. *Cell* **112:** 407–421

Davidson G, Shen J, Huang YL, Su Y, Karaulanov E, Bartscherer K, Hassler C, Stannek P, Boutros M, Niehrs C (2009) Cell cycle control of wnt receptor activation. *Dev Cell* **17:** 788–799

Davidson G, Wu W, Shen J, Bilic J, Fenger U, Stannek P, Glinka A, Niehrs C (2005) Casein kinase 1γ couples Wnt receptor activation to cytoplasmic signal transduction. *Nature* **438:** 867–872

Dephoure N, Zhou C, Villén J, Beausoleil SA, Bakalarski CE, Elledge SJ, Gygi SP (2008) A quantitative atlas of mitotic phosphorylation. *Proc Natl Acad Sci USA* **105:** 10762–10767

Draviam VM, Shapiro I, Aldridge B, Sorger PK (2006) Misorientation and reduced stretching of aligned sister kinetochores promote chromosome missegregation in EB1- or APC-depleted cells. *EMBO J* **25:** 2814–2827

Elia AE, Cantley LC, Yaffe MB (2003) Proteomic screen finds pSer/pThr-binding domain localizing Plk1 to mitotic substrates. *Science* **299:** 1228–1231

Elowe S, Hummer S, Uldschmid A, Li X, Nigg EA (2007) Tension-sensitive Plk1 phosphorylation on BubR1 regulates the stability of kinetochore microtubule interactions. *Genes Dev* **21:** 2205–2219

Feng J, Huang H, Yen TJ (2006) CENP-F is a novel microtubule-binding protein that is essential for kinetochore attachments and affects the duration of the mitotic checkpoint delay. *Chromosoma* **115:** 320–329

Fumoto K, Lee PC, Saya H, Kikuchi A (2008) AIP regulates stability of Aurora-A at early mitotic phase coordinately with GSK-3β. *Oncogene* **27:** 4478–4487

Green JL, Kuntz SG, Sternberg PW (2008) Ror receptor tyrosine kinases: orphans no more. *Trends Cell Biol* **18:** 536–544

Hadjihannas MV, Bruckner M, Jerchow B, Birchmeier W, Dietmaier W, Behrens J (2006) Aberrant Wnt/β-catenin signaling can induce chromosomal instability in colon cancer. *Proc Natl Acad Sci USA* **103:** 10747–10752

Izumi N, Fumoto K, Izumi S, Kikuchi A (2008) GSK-3β regulates proper mitotic spindle formation in cooperation with a component of the γ-tubulin ring complex, GCP5. *J Biol Chem* **283:** 12981–12991

Jelluma N, Brenkman AB, McLeod I, Yates III JR, Cleveland DW, Medema RH, Kops GJ (2008a) Chromosomal instability by inefficient Mps1 auto-activation due to a weakened mitotic checkpoint and lagging chromosomes. *PLoS One* **3:** e2415

Jelluma N, Brenkman AB, van den Broek NJ, Cruijsen CW, van Osch MH, Lens SM, Medema RH, Kops GJ (2008b) Mps1 phosphorylates Borealin to control Aurora B activity and chromosome alignment. *Cell* **132:** 233–246

Kang J, Chen Y, Zhao Y, Yu H (2007) Autophosphorylation-dependent activation of human Mps1 is required for the spindle checkpoint. *Proc Natl Acad Sci USA* **104:** 20232–20237

Kaplan KB, Burds AA, Swedlow JR, Bekir SS, Sorger PK, Näthke IS (2001) A role for the Adenomatous Polyposis Coli protein in chromosome segregation. *Nat Cell Biol* **3:** 429–432

Kawano Y, Kypta R (2003) Secreted antagonists of the Wnt signalling pathway. *J Cell Sci* **116:** 2627–2634

Kikuchi A, Yamamoto H, Sato A (2009) Selective activation mechanisms of Wnt signaling pathways. *Trends Cell Biol* **19:** 119–129

Kiyomitsu T, Obuse C, Yanagida M (2007) Human Blinkin/AF15q14 is required for chromosome alignment and the mitotic checkpoint through direct interaction with Bub1 and BubR1. *Dev Cell* **13:** 663–676

Kline-Smith SL, Walczak CE (2004) Mitotic spindle assembly and chromosome segregation: refocusing on microtubule dynamics. *Mol Cell* **15:** 317–327

Kurayoshi M, Oue N, Yamamoto H, Kishida M, Inoue A, Asahara T, Yasui W, Kikuchi A (2006) Expression of Wnt-5a is correlated with aggressiveness of gastric cancer by stimulating cell migration and invasion. *Cancer Res* **66:** 10439–10448

Lampson MA, Kapoor TM (2005) The human mitotic checkpoint protein BubR1 regulates chromosome-spindle attachments. *Nat Cell Biol* **7:** 93–98

Lane HA, Nigg EA (1996) Antibody microinjection reveals an essential role for human polo-like kinase 1 (Plk1) in the functional maturation of mitotic centrosomes. *J Cell Biol* **135:** 1701–1713

Lee YN, Gao Y, Wang HY (2008) Differential mediation of the Wnt canonical pathway by mammalian Dishevelleds-1, -2, and -3. *Cell Signal* **20:** 443–452

Lénárt P, Petronczki M, Steegmaier M, Di Fiore B, Lipp JJ, Hoffmann M, Rettig WJ, Kraut N, Peters JM (2007) The small-molecule inhibitor BI 2536 reveals novel insights into mitotic roles of polo-like kinase 1. *Curr Biol* **17:** 304–315

Liu ST, Chan GK, Hittle JC, Fujii G, Lees E, Yen TJ (2003) Human MPS1 kinase is required for mitotic arrest induced by the loss of CENP-E from kinetochores. *Mol Biol Cell* **14:** 1638–1651

Logan CY, Nusse R (2004) The Wnt signaling pathway in development and disease. *Annu Rev Cell Dev Biol* **20:** 781–810

MacDonald BT, Tamai K, He X (2009) Wnt/β-catenin signaling: components, mechanisms, and diseases. *Dev Cell* **17:** 9–26

Matsumoto S, Fumoto K, Okamoto T, Kaibuchi K, Kikuchi A (2010) Binding of APC and dishevelled mediates Wnt5a-regulated focal adhesion dynamics in migrating cells. *EMBO J* **29:** 1192–1204

Matsumura S, Toyoshima F, Nishida E (2007) Polo-like kinase 1 facilitates chromosome alignment during prometaphase through BubR1. *J Biol Chem* **282:** 15217–15227

McCartney BM, Näthke IS (2008) Cell regulation by the Apc protein Apc as master regulator of epithelia. *Curr Opin Cell Biol* **20:** 186–193

Meraldi P, Sorger PK (2005) A dual role for Bub1 in the spindle checkpoint and chromosome congression. *EMBO J* **24:** 1621–1633

Musacchio A, Salmon ED (2007) The spindle-assembly checkpoint in space and time. *Nat Rev Mol Cell Biol* **8:** 379–393

Niehrs C (2006) Function and biological roles of the Dickkopf family of Wnt modulators. *Oncogene* **25:** 7469–7481

Niikura Y, Ohta S, Vandenbeldt KJ, Abdulle R, McEwen BF, Kitagawa K (2006) 17-AAG, an Hsp90 inhibitor, causes kinetochore defects: a novel mechanism by which 17-AAG inhibits cell proliferation. *Oncogene* **25:** 4133–4146

Oshimori N, Ohsugi M, Yamamoto T (2006) The Plk1 target Kizuna stabilizes mitotic centrosomes to ensure spindle bipolarity. *Nat Cell Biol* **8:** 1095–1101

Petronczki M, Lénárt P, Peters JM (2008) Polo on the rise-from mitotic entry to cytokinesis with Plk1. *Dev Cell* **14:** 646–659

Piehl M, Tulu US, Wadsworth P, Cassimeris L (2004) Centrosome maturation: measurement of microtubule nucleation throughout the cell cycle by using GFP-tagged EB1. *Proc Natl Acad Sci USA* **101:** 1584–1588

Purro SA, Ciani L, Hoyos-Flight M, Stamatakou E, Siomou E, Salinas PC (2008) Wnt regulates axon behavior through changes in microtubule growth directionality: a new role for adenomatous polyposis coli. *J Neurosci* **28:** 8644–8654

Sakane H, Yamamoto H, Kikuchi A (2010) LRP6 is internalized by Dkk1 to suppress its phosphorylation in the lipid raft and is recycled for reuse. *J Cell Sci* **123:** 360–368

Santamaria A, Neef R, Eberspacher U, Eis K, Husemann M, Mumberg D, Prechtl S, Schulze V, Siemeister G, Wortmann L, Barr FA, Nigg EA (2007) Use of the novel Plk1 inhibitor ZK-thiazolidinone to elucidate functions of Plk1 in early and late stages of mitosis. *Mol Biol Cell* **18:** 4024–4036

Sato A, Yamamoto H, Sakane H, Koyama H, Kikuchi A (2010) Wnt5a regulates distinct signalling pathways by binding to Frizzled2. *EMBO J* **29:** 41–54

Sillje HH, Nagel S, Korner R, Nigg EA (2006) HURP is a Ran-importin β-regulated protein that stabilizes kinetochore microtubules in the vicinity of chromosomes. *Curr Biol* **16:** 731–742

Stucke VM, Sillje HH, Arnaud L, Nigg EA (2002) Human Mps1 kinase is required for the spindle assembly checkpoint but not for centrosome duplication. *EMBO J* **21:** 1723–1732

Sumara I, Gimenez-Abian JF, Gerlich D, Hirota T, Kraft C, de la Torre C, Ellenberg J, Peters JM (2004) Roles of polo-like kinase 1 in the assembly of functional mitotic spindles. *Curr Biol* **14:** 1712–1722

Tanaka TU, Stark MJ, Tanaka K (2005) Kinetochore capture and bi-orientation on the mitotic spindle. *Nat Rev Mol Cell Biol* **6:** 929–942

Taylor SS, McKeon F (1997) Kinetochore localization of murine Bub1 is required for normal mitotic timing and checkpoint response to spindle damage. *Cell* **89:** 727–735

Tetsu O, McCormick F (1999) β-Catenin regulates expression of cyclin D1 in colon carcinoma cells. *Nature* **398:** 422–426

Thoma CR, Toso A, Gutbrodt KL, Reggi SP, Frew IJ, Schraml P, Hergovich A, Moch H, Meraldi P, Krek W (2009) VHL loss causes

spindle misorientation and chromosome instability. *Nat Cell Biol* **11:** 994–1001

Toyoshima F, Nishida E (2007) Integrin-mediated adhesion orients the spindle parallel to the substratum in an EB1- and myosin X-dependent manner. *EMBO J* **26:** 1487–1498

Uchida KS, Takagaki K, Kumada K, Hirayama Y, Noda T, Hirota T (2009) Kinetochore stretching inactivates the spindle assembly checkpoint. *J Cell Biol* **184:** 383–390

van Vugt MA, van de Weerdt BC, Vader G, Janssen H, Calafat J, Klompmaker R, Wolthuis RM, Medema RH (2004) Polo-like kinase-1 is required for bipolar spindle formation but is dispensable for anaphase promoting complex/Cdc20 activation and initiation of cytokinesis. *J Biol Chem* **279:** 36841–36854

Vigneron S, Prieto S, Bernis C, Labbe JC, Castro A, Lorca T (2004) Kinetochore localization of spindle checkpoint proteins: who controls whom? *Mol Biol Cell* **15:** 4584–4596

Walston T, Tuskey C, Edgar L, Hawkins N, Ellis G, Bowerman B, Wood W, Hardin J (2004) Multiple Wnt signaling pathways converge to orient the mitotic spindle in early C. elegans embryos. *Dev Cell* **7:** 831–841

Wharton KAJ (2003) Runnin' with the Dvl: proteins that associate with Dsh/Dvl and their significance to Wnt signal transduction. *Dev Biol* **253:** 1–17

Xue Y, Zhou F, Zhu M, Ahmed K, Chen G, Yao X (2005) GPS: a comprehensive www server for phosphorylation sites prediction. *Nucleic Acids Res* **33:** W184–W187

Yamamoto H, Sakane H, Yamamoto H, Michiue T, Kikuchi A (2008) Wnt3a and Dkk1 regulate distinct internalization pathways of LRP6 to tune the activation of β-catenin signaling. *Dev Cell* **15:** 37–48

Yasuda S, Oceguera-Yanez F, Kato T, Okamoto M, Yonemura S, Terada Y, Ishizaki T, Narumiya S (2004) Cdc42 and mDia3 regulate microtubule attachment to kinetochores. *Nature* **428:** 767–771

Yu H (2007) Cdc20: a WD40 activator for a cell cycle degradation machine. *Mol Cell* **27:** 3–16